Correcting the Dipole Cascade with Matrix Elements in Hadron Collisions

Nils Lavesson*
Master of Science Thesis

Thesis Advisor: Leif Lönnblad †
Department of Theoretical Physics: Lund University
Sölvegatan 14A, S-22362 Lund, Sweden

March 19, 2004

Abstract

There are two main ways of describing multi particle production: fixed order matrix elements and parton showers. They provide a good description in complementary regions of phase space. There is an algorithm available for correcting the dipole cascade model with fixed order matrix elements in e^+e^- collisions[1]. This algorithm is modified to be used for hadron-hadron collision in general and W^+ production in proton antiproton collisions at the Tevatron in particular.

*f99nl@efd.lth.se
†leif@thep.lu.se

Contents

1 Introduction

During the last few decades particle physicists have constructed a model describing almost all experimental results, known as the standard model. This model includes the electromagnetic force, the weak force and the strong force, but not yet gravity. The theory is rather complex and it is not trivial to go from theory to experimental predictions. This paper will show how one aspect of experimental predictions in quantum chromo dynamics can be improved.

Quantum Chromo Dynamics (QCD) is the theory in particle physics that describes the strong interaction. The strong interaction is a short range interaction noticeable only on the femtometer scale, but at short distances it is much stronger than all the other forces of nature. The strong interaction is the force that binds the quarks together in a hadron and the nucleons together in an atomic nucleus.

QCD only acts on quarks and gluons and is mediated by gluons. The charges in QCD are called colors and are labeled red, blue, green and their anticolors, giving a total of six charges. Quarks carry color charge, antiquarks carry anticolor charge and the gluons carry both color and anticolor charge. Contrary to the electromagnetic interaction the mediators of the strong force carry charge themselves.

The strength of QCD is determined by the strong coupling constant α_s. The coupling constant is dependent on the resolution of the process. High resolution requires high energy in accordance with the de Broglie wavelength. The quantity used to measure this is the virtuality of a process, typically denoted Q^2, defined as the invariant mass squared of the mediated particle, in this case the gluon. The virtuality dependence of α_s is to leading order given by:

$$\alpha_\mathrm{s}(Q^2) = \frac{12\pi}{(33 - 2n_f)\ln(Q^2/\Lambda^2_{\mathrm{QCD}})} \tag{1}$$

n_f is the number of available quark flavors which is between two and six and Λ_{QCD} ($\approx 200MeV$) is the fundamental scale of QCD which needs to be measured experimentally.

Two other important properties of QCD are those of asymptotic freedom and confinement. Asymptotic freedom refers to the fact that the strength of the strong force decreases in the high virtuality limit, which makes the partons essentially free. Confinement is the property of QCD which states that only

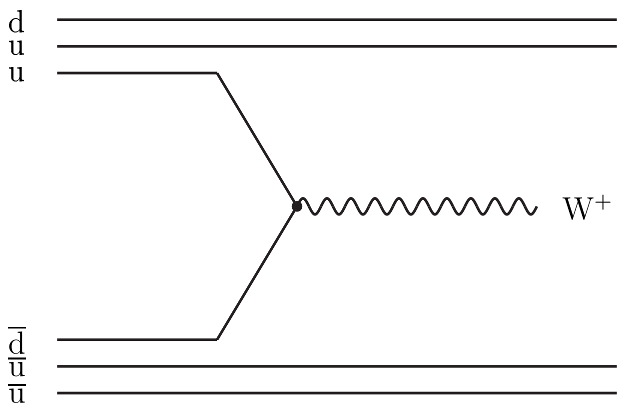

Figure 1: Lowest order W^+ production in proton antiproton collision.

color neutral objects, known as hadrons, can be observed, while free quarks can never be detected. Hadrons are bound states consisting of several quarks and/or antiquarks. If a quark is given enough energy to leave a hadron, the energy in the color field will grow, which will result in the production of quark-antiquark pairs and the formation of new hadrons. The hadrons produced in a particle collision tend to follow the direction of an initial hard parton forming a shower of particles known as a jet.

Most processes in high energy physics can be described by Feynman diagrams. Quarks and other fermions are represented by straight lines and gluons and other bosons by curly lines. The coupling in each point is described by a coupling constant. The diagram in figure 1 shows the simplest possible diagram for producing a W^+ in a proton-antiproton collision.

There are three different methods that need to be combined in order to give the best possible description of QCD processes. In the high virtuality limit QCD processes are best described by fixed order matrix elements, in the medium virtuality range parton showers give the best description and in the low virtuality region hadronization models describe the transition into observable hadrons.

The complexity of these models makes it very difficult to do any analytical calculations. Instead Monte Carlo techniques are used. Computer programs, called Monte Carlo event generators, are implemented to generate random events in accordance with the models. The output of such a program can then be compared with experimental results.

This paper will describe a method for correcting the dipole cascade model with fixed order matrix elements in a consistent way in the Monte Carlo event generator ARIADNE for hadronic collisions. In particular production of W-bosons together with hard jets is studied because it is a major background to Higgs and top production. When doing experiments with both Higgs and top production, the background is minimized using the correlation between jets. This is not well simulated in parton cascades without matrix element corrections. To evaluate the background properly algorithms of the type presented are needed.

The outline of the paper is the following. Section 2 will explain some of general properties of quantum chromo dynamics. Then in section 3 the color dipole cascade model will be explained, followed by the algorithm used to implement matrix element corrections in section 4. Some preliminary results are presented in section 5.

2 Quantum Chromo Dynamics

2.1 Matrix Elements

In QCD or any other quantum field theory the probability of a specific process is proportional to a matrix element squared. For a small coupling matrix elements can be expanded in powers of α_s. These calculations are exact up to the calculated order.

The convergence of such an expansion depends on α_s being small and that the coefficients remain small. The expansion does not work in the low energy and collinear region. In both these regions the virtuality is very low, which makes α_s become close to one, but even if α_s remains small the large phase space gives rise to large logarithmic terms. This causes the expansion to break down.

It is therfore vital to introduce a cutoff. In this article the $k_\perp$-clustering algorithm[7], described below, is used as the cutoff. This introduces a cutoff both in the collinear and the infrared (low energy) region, which ensures the convergence of the α_s expansion.

There exist different schemes for generating Monte Carlo events from matrix elements. The events used in this analysis were generated by MadGraph [9] which is a tree-level diagram generator, which means that no loop diagrams are included. MadGraph works by constructing all possible diagrams for a specific process and calls HELAS[10] to calculate the amplitudes of the different diagrams.

2.2 Parton cascades

Parton cascades are constructed by studying diagrams where an order in virtuality can be established, in other words when each vertex has a much higher virtuality than the next. In this limit the matrix elements approximately factorize into splitting functions, one for each vertex, which are dominated by large logarithmic contributions from the soft and collinear poles. Keeping only the leading order logarithm is known as leading log approximation (LLA), which is the foundation for all parton cascade models. There are other approximations available that also include some nonleading contributions known as modified leading log approximation (MLLA).

The leading logarithm is a good approximation for the divergent parts of the QCD process. This turns out to be the dominant contribution for the entire QCD process, which makes it reasonable to use the cascade to simulate the entire process.

Since the matrix elements factorize, each vertex can be considered to be independent. This makes the parton cascade suitable for computer implementations since it can be done step by step.

The disadvantage of using parton cascades is that the correlations between the different partons are not very well approximated. In particular states with several hard widely separated partons are poorly described with cascades.

In this article the parton cascade used is the dipole cascade [3] as implemented in the program ARIADNE [2]. The cascade is described in section 3.

2.3 Hadronization

At even lower virtuality the perturbative approach breaks down completely. At these scales nonperturbative models are needed. In particular a nonperturbative model is needed to describe the transitions to hadrons.

There are several models available that accomplish this. The most commonly used is the Lund Model[6]. The Lund model states that the color field form tubes, which are approximated as massless relativistic strings. At low energy the strings fragment forming quark antiquark pairs that become part of new hadrons. These hadrons have a tendency to be emitted in the same directions as a hard parton in the underlying partonic structure of the event. When a hard parton is present in the event this can be seen by a large amount of energy present in the form of hadrons in a small angular region, which is known as a jet.

Hadronization models have not been used in this paper but would be relevant for further studies.

2.4 Jet Clustering

When a QCD event occurs in a collider the observed final state consists of a large number of hadrons. In order to get an idea of the underlying partonic structure of the event, jet clustering algorithms are used. Jet clustering algorithm use different methods to cluster a number of particles together in one entity called a jet, which is correlated to a high energetic parton in the event.

The $k_\perp$-clustering algorithm[7], used throughout this paper, defines a resolution variable to identify which particles lie close in phase space. The resolution variable takes into account both the energy of the particles and the angle between them. The algorithm takes the two particles that have the lowest value of the resolution variable and clusters them together to one pseudoparticle. In hadron-hadron collision an additional clustering is possible namely to cluster a particle with the beam and an associated resolution variable is defined for this purpose. The idea is to cluster all of the particles that lie close to the beam into a jet associated with the hadron remnants. The algorithm continues until all the (pseudo)particles are separated by a resolution variable bigger than a cutoff.

The $k_\perp$-clustering algorithm comes with a number of choices of how to define the resolution variable and how to cluster two (pseudo)particles into a new pseudoparticle. All the choices of resolution variable have the same properties in the small angle limit.

$$\begin{aligned} d_{kB} &= E_k^2\theta_{kB}^2 \quad for \quad \theta_{kB} \to 0 \\ d_{kl} &= \min(E_k^2, E_l^2)\theta_{kl}^2 \quad for \quad \theta_{kl} \to 0 \end{aligned} \tag{2}$$

The indices k and l refer to particles and B to the beam. These equations have an energy and angle dependence that makes them safe to use in the region where the emission probability diverges, which are the collinear and infrared regions. These properties make the algorithm suitable to define matrix element cutoffs.

In this article the covariant E-scheme is used. This scheme has the advantage of being boost invariant along the beam axis. The resolution variables are defined in the following way.

$$\begin{aligned} d_{kB} &= p_{\perp k}^2 \\ d_{kl} &= \min(p_{\perp k}^2, p_{\perp l}^2)((\eta_k - \eta_l)^2 + (\phi_k - \phi_l)^2) \end{aligned} \tag{3}$$

$p_\perp$ is the tranverse momenta and η is the pseudorapidity defined as $\eta = -\ln\tan\frac{\theta}{2}$. Equations (3) reproduces equations (2) in the small angle limit. Particles are combined into pseudo particles by adding their momentum.

$$p_{(ij)} = p_i + p_j \tag{4}$$

Since the pseudoparticles created this way are not massless, the rapidity, defined as $y = \frac{1}{2}\ln(\frac{E+p_z}{E-p_z})$, is used instead of the pseudorapidity. In this manner the boost invariance along the beam axis is maintained.

If the same jet clustering algorithm is used to determine the cutoff for the matrix elements as to look at the final state, a nice comparison can be made. There are effects from hadronization which will add some distortions, but hadronization is not studied in this report.

2.5 Parton Distribution

The proton is a complex object. It not only contains three valence quarks but also includes gluons and sea quarks. Gluons are created in the interactions between the valence quarks and sea quarks are created when a gluon fluctuates into a virtual quark antiquark pair. How many of these structures that can be seen experimentally depends on the resolution at which the proton is probed. In other words it depends on how high the virtuality of the process is. These properties are of great importance when studying hadron collisions, since they dictate the likelihood of a particular parton to be present in the interaction and how big part of the total proton momentum the specific parton is carrying.

All of these properties can be described by the parton distributions of the proton. The parton distribution describe the density of a given parton with a given momentum when probed with a given virtuality.

Parton distribution functions are denoted $f_{q/p}(x, Q^2)$ where q is the flavor of the parton and x is the momentum fraction. The notation xf is used to refer to the density in the logarithmic momentum fraction, hence $xf_{q/p}(x', Q^2) = x' \cdot f_{q/p}(x', Q^2)$.

The evolution in Q^2 of the distribution is known from perturbative QCD, but the starting point of the evolution at low virtuality cannot be calculated. Parameterizations are therefore used to describe the low virtuality distributions and the parameters are measured experimentally by fitting the evolved high virtuality distributions to data. In this article the CTEQ6 parton distributions are used[8].

3 The Color Dipole Cascade Model

The color dipole cascade model (CDM)[3] is based on the idea of describing the parton cascade radiation, as radiation of gluons from a color dipole formed between two partons. This differs from conventional parton showers in that instead of having partonic splittings of the type $1 \rightarrow 2$, the diplole cascade model is based on $2 \rightarrow 3$ partonic processes. Another difference is that in hadronic collisions conventional parton showers use both initial state and final state radiation but in the dipole picture all gluon emissions are treated as final state radiation.

A dipole cascade may start with one dipole between a quark antiquark pair that radiates a gluon, which has color and anticolor charge and therefore forms part of two new quark gluon dipoles. Each of these dipoles may continue radiating independently creating new dipoles until a cutoff is reached. Below this cutoff hadronization models describe the transitions to hadrons.

3.1 Gluon Radiation

There are three basic types of dipoles: quark-antiquark, quark-gluon, and gluon-gluon. All the dipoles can radiate a gluon. The splitting functions are defined in terms of x_i which are the final state energy fractions:

$$x_i = \frac{2E_i}{\sqrt{s_{dip}}} \tag{5}$$

E_i is the energy of the outgoing parton in the dipole center of mass frame and s_{dip} is the invariant mass squared of the dipole. All the relevant Feynman

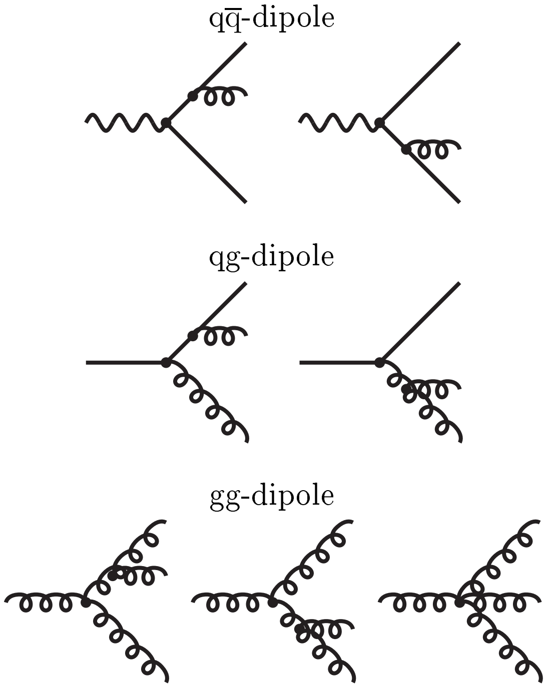

Figure 2: Feynman diagram for the three types of dipoles radiating a gluon.

diagrams are shown in figure 2. The dipole splitting functions are calculated from the corresponding diagrams including interference terms. The results are:

$$P^{dip}_{\mathrm{q\overline{q}}} = \frac{2\alpha_{\mathrm{s}}}{3\pi}\frac{x_1^2+x_3^2}{(1-x_1)(1-x_3)} \tag{6}$$

$$P^{dip}_{\mathrm{qg}} = \frac{3\alpha_{\mathrm{s}}}{4\pi}\frac{x_1^3+x_3^2}{(1-x_1)(1-x_3)} \tag{7}$$

$$P^{dip}_{\mathrm{gg}} = \frac{3\alpha_{\mathrm{s}}}{4\pi}\frac{x_1^3+x_3^3}{(1-x_1)(1-x_3)} \tag{8}$$

The splitting functions specify the energy fractions of the emitted partons, which can be used to determine the angles between the partons. There are two more degrees of freedom, not given by theory, that need to be taken into account, which are the azimuth angle ϕ and the polar angle θ. In ARIADNE the following choices are made: The azimuth angle ϕ is taken to be evenly distributed between 0 and 2π. The polar angle, defined in figure 3, is distributed differently for different dipoles. If a quark-antiquark pair emits a gluon, a quark retains its direction with a probability proportional to the

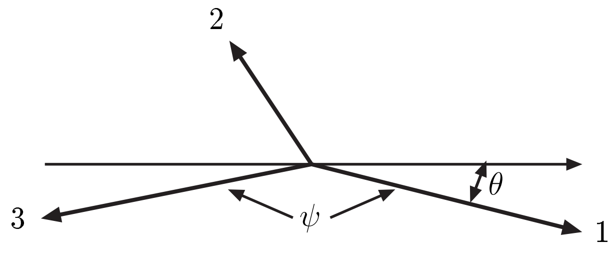

Figure 3: The dipole after an emission.

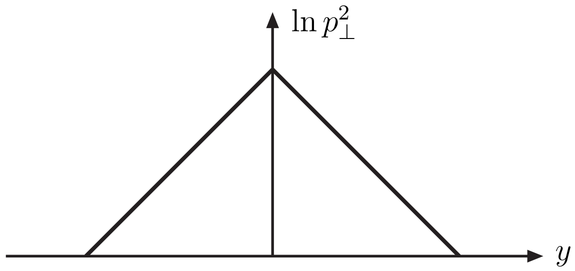

Figure 4: The available phase space of an emitted gluon.

square of its energy. In other kinds of emissions the idea is that the disturbance of the color flow in connected dipoles should be minimized. This is implemented by giving all the recoil to the quark in a quark-gluon dipole and to distribute the recoil in a gluon-gluon dipole according to the following formula:

$$\theta = \frac{x_3^2}{x_1^2 + x_3^2}(\pi - \psi) \tag{9}$$

3.2 Energy Scale

All the emissions within the color dipole cascade model are described in terms of the two phase space variables: the invariant $p_\perp^2$ and y defined as:

$$\begin{aligned} p_\perp^2 &= s_{dip}\left(1 - x_1 + \frac{m_1^2 - (m_2+m_3)^2}{s_{dip}}\right) \cdot \\ &\quad \left(1 - x_3 + \frac{m_3^2 - (m_1+m_2)^2}{s_{dip}}\right) \end{aligned} \tag{10}$$

$$y = \frac{1}{2}\ln\left(\frac{1-x_1}{1-x_3}\right) \quad (11)$$

s_{dip} is the invariant mass squared of the dipole. $p_\perp^2$ is also used to define the virtuality of an emission. For massless particle the available phase space of the gluon emission is $p_\perp < \frac{\sqrt{s_{dip}}}{e^y+e^{-y}}$ approximately described by the triangle shown in figure 4.

When transformed into the new coordinates $p_\perp^2$ and y, it can be shown that all the splitting functions are well approximated by the following proportionality:

$$P^{dip}dx_1dx_3 \propto \alpha_s \frac{dp_\perp^2}{p_\perp^2}dy \quad (12)$$

This is a convenient choice of coordinates since the emission probability is almost flat in rapidity and $\log p_\perp^2$.

3.3 Ordering

Since $p_\perp^2$ is used to define the virtuality of an emission it is also used to order the emissions. This means that an emission at a scale $p_{\perp 1}^2$ is performed before an emission at a lower scale $p_{\perp 2}^2 < p_{\perp 1}^2$. This is accomplished by introducing a Sudakov form factor in the emission probability. The probability of an emission is described by the following formula:

$$P(p_\perp^2, y) = P^{dip}(p_\perp^2, y)e^{-\int_{p_\perp^2}^{p_{\perp max}^2}\int_{y_{min(p_\perp'^2)}}^{y_{max(p_\perp'^2)}} dy' dp_\perp'^2 P^{dip}(p_\perp'^2, y')} \quad (13)$$

The first part of the probability is the dipole splitting functions and the second part is the so called Sudakov form factor. This factor is the probability that no emission has occurred at a scale higher than $p_\perp^2$.

The CDM is a modified leading log approximation (MLLA). It can be proven to be a good approximation in the limit of strongly ordered emissions in $p_\perp^2$. It is kinematically possible to have an emission at a scale $p_\perp^2$ followed by an emission at a slightly higher scale, if all the dipoles are considered to be independent. In ARIADNE however all the emissions are required to be strictly ordered.

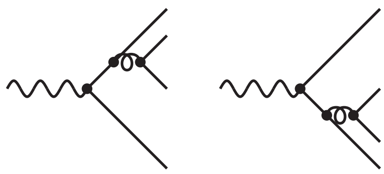

Figure 5: The Feynman diagrams for $Q\overline{Q}$ production.

3.4 $Q\overline{Q}$ Production

The process of a gluon splitting into a quark antiquark pair needs to be added to the dipole picture. The process is not as straight forward to implement as the gluon emission. The splitting function is calculated by studying the diagrams for $q\overline{q} \to q\overline{q}Q\overline{Q}$ shown in figure 5. It can be shown that in the limit of $m_{Q\overline{Q}} \ll p_{\perp g}$ the splitting function can be factorized into two parts, where one factor represents the process $q\overline{q} \to qg\overline{q}$ and one represents $g \to Q\overline{Q}$. If half of the later is associated to each of the dipoles connected to the gluon the following splitting function is obtained:

$$P^{dip}_{qg \to qQ\overline{Q}} = \frac{\alpha_s}{8\pi} \frac{(1-x_2)^2 + (1-x_3)^2}{(1-x_1)} \tag{14}$$

2 and 3 refers to $Q\overline{Q}$ pair.

3.5 Emission from an extended source

When a hard partonic interaction occurs in hadronic collisions, dipoles are formed between these partons and remnants from hadrons in the beams. The remnant from the beam is not a point-like particle, however, and this needs to be taken into account when considering the radiation from such a dipole[4].

With an extended source taking part in a dipole emission, radiation with a small wavelength will not be able to resolve the entire remnant structure. This is implemented in a way where only part of the remnant takes part in the emission.

$$a = \left(\frac{\mu}{p_\perp}\right)^\alpha \tag{15}$$

The parameter a is the fraction of the proton remnant that can be resolved by the emitted gluon. μ describes the inverse size and α the number of

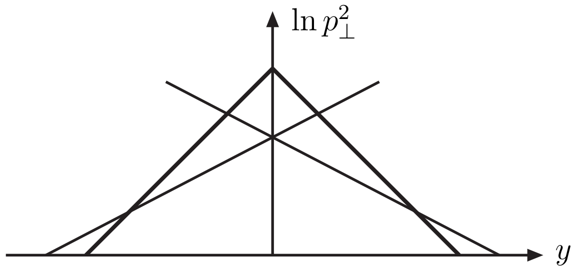

Figure 6: The available phase space of an emitted gluon from two extended sources. The two extra lines represent the restrictions from the extendedness of the constituents in the dipole.

dimensions of the extended particle. This leads to an extra restriction on the available phase space illustrated in figure 6.

For practical purposes a soft cutoff is used which allows emissions above the sharp cutoff in equation (15).

$$\frac{dP(a')}{da'} = \frac{b}{a}\frac{(\frac{a'}{a})^{-1}}{(1+(\frac{a'}{a})^b)^2} \tag{16}$$

This is the probability that a fraction a' takes part in the emission. The variable a is the sharp cutoff from equation (15) and b is a tuning parameter normally set to two. This corresponds to an exponential suppression above the cutoff in $lnp_\perp^2, y$ coordinates.

There is one additional property of extended particles namely that transverse momentum is never given to them. Instead it is either given to the W boson or to a so-called recoil gluon created specifically to absorb the recoil.

3.6 Sea Quark Emission

Another process that must to be added to the dipole cascade when studying hadron collisions is that of initial state $\mathrm{g} \to \mathrm{q}\overline{\mathrm{q}}$ splitting. In the dipole cascade model this process is represented by a proton remnant dipole which emits a sea quark[5]. The process is therefore referred to as a sea quark emission which is shown in figure 7.

The process cannot be described within terms of ordinary dipoles. Instead it is considered to be an emission from the proton remnant alone, but the

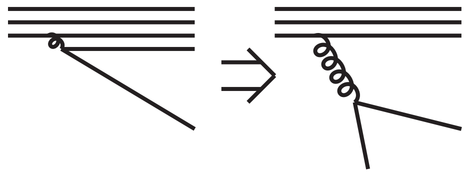

Figure 7: Diagrams showing a sea quark emission.

transverse recoil cannot be given to the proton remnant and is therefore added to the hard system containing all nonextended particles in the collision. The invariant $p_\perp^2$ (equation (11)) is not defined for this type of a process, instead the real $p_\perp^2$ of the emitted antiquark is used. The splitting function for the process given by:

$$dP_q^{dip} = \frac{\alpha_\mathrm{s}}{4\pi}(z^2 + (1-z)^2)(1-z)\frac{xf_g(x/z, p_\perp^2)}{xf_q(x, p_\perp^2)}\frac{dp_\perp^2}{p_\perp^2}dy \tag{17}$$

x is the momentum fraction of the sea quark initially taken from the proton and z is a function of $p_\perp^2$ and y representing the momentum fraction of the sea quark divided by that of the gluon.

4 Combining ME with CDM

As described earlier the two methods of parton cascades and matrix elements are working well in different parts of phase space. A combination of the models is needed to give the best possible result. The two methods should not be allowed to generate emissions in the same region of phase space, nor should there be any regions of phase space where neither model generates emissions. The two models have been successfully combined in the e^+e^- case[1].

4.1 Matrix Elements and Sudakov Form Factors

Matrix elements can be expanded up to a given order in α_s. The ratios for W plus 0, 1 and 2 jet production in an proton antiproton collision up to order

α_s^2 with a cutoff Q_0 can be written as:

$$\begin{aligned}
R_0(Q_{max}, Q_0) &= 1 + \alpha_s C_{0,1}(Q_{max}, Q_0) + \alpha_s^2 C_{0,2}(Q_{max}, Q_0) &(18)\\
R_1(Q_{max}, Q_0) &= \alpha_s C_{1,1}(Q_{max}, Q_0)(1 + \alpha_s C_{1,2}(Q_{max}, Q_0)) &(19)\\
R_2(Q_{max}, Q_0) &= \alpha_s^2 C_{2,2}(Q_{max}, Q_0) &(20)
\end{aligned}$$

The coefficients $C_{a,b}$ are calculated from perturbation theory. The expansion has to be cut off at an energy scale Q_0 to avoid divergencies in the matrix elements.

In the color dipole cascade framework the probability of a W plus no jet event can be written in the form of a Sudakov form factor, which can be expanded in terms of α_s. This is the probability that no emission occurs throughout the cascade.

$$\begin{aligned}
R_0(p^2_{\perp max}, p^2_{\perp min}) &= \Delta_{S_0}(p^2_{\perp max}, p^2_{\perp min})\\
&= \exp\left(-\int_{p^2_{\perp min}}^{p^2_{\perp max}}\int_{y_{min}}^{y_{max}} dy dp^2_\perp P^{dip}\right) &(21)\\
R_0(p^2_{\perp max}, p^2_{\perp min}) &= 1 + \alpha_s C^{PS}_{0,1}(p^2_{\perp max}, p^2_{\perp min}) +\\
&\quad \alpha_s^2 C^{PS}_{0,2}(p^2_{\perp max}, p^2_{\perp min}) + ... &(22)
\end{aligned}$$

Δ_{S_0} denotes the probability that a state S_0 doesn't emit any partons between the two given scales.

In the same manner the equations for higher jet multiplicity can be constructed. This is what the equations look like for W plus one jet events, which can also be expanded in terms of α_s.

$$\begin{aligned}
R_1(p^2_{\perp max}, p^2_{\perp min}) &= \int_{p^2_{\perp min}}^{p^2_{\perp max}}\int_{y_{min}}^{y_{max}} dy dp^2_\perp P^{dip} \cdot\\
&\quad \Delta_{S_0}(p^2_{\perp max}, p^2_\perp)\Delta_{S_1}(p^2_\perp, p^2_{\perp min}) &(23)\\
R_1(p^2_{\perp max}, p^2_{\perp min}) &= \alpha_s C^{PS}_{1,1}(p^2_{\perp max}, p^2_{\perp min}) \cdot\\
&\quad (1 + \alpha_s C^{PS}_{1,2}(p^2_{\perp max}, p^2_{\perp min}) + ...) &(24)
\end{aligned}$$

The W plus one jet probability is the probability of having an emission at a scale $p^2_\perp$ multiplied by the probability of not having any emission at a higher nor at a lower scale, which is integrated over the entire phase space. The equations for W plus two jets can be written in the following way:

$$R_2(p^2_{\perp max}, p^2_{\perp min}) = \int_{p^2_{\perp min}}^{p^2_{\perp max}}\int_{y_{min}}^{y_{max}} dy_1 dp^2_{\perp 1} P^{dip}(p^2_{\perp 1}, y_1) \cdot$$

$$
\begin{aligned}
& \int_{p^2_{\perp min}}^{p^2_{\perp 1}} \int_{y_{min}}^{y_{max}} dy_2 dp^2_{\perp 2} P^{dip}(p^2_{\perp 2}, y_2) \cdot \\
& \Delta_{S_0}(p^2_{\perp max}, p^2_{\perp 1}) \Delta_{S_1}(p^2_{\perp 1}, p^2_{\perp 2}) \cdot \\
& \Delta_{S_2}(p^2_{\perp 2}, p^2_{\perp min}) \qquad (25) \\
R_2(p^2_{\perp max}, p^2_{\perp min}) = \; & \alpha_s^2 C^{PS}_{2,2}(p^2_{\perp max}, p^2_{\perp min}) \cdot \\
& (1 + \alpha_s C^{PS}_{2,3}(p^2_{\perp max}, p^2_{\perp min}) + ...) \qquad (26)
\end{aligned}
$$

The idea when combining the two methods is to replace the multiplication of splitting functions with the full matrix element in the part of phase space where the matrix element works better. The matrix elements are generated using a tree-level generator, which means that only the terms $C_{i,j}$ where $i = j$ are calculated. Higher order terms are introduced via the parton cascade.

4.2 Reconstruction of Emissions

Events generated in accordance with matrix elements need to be reweighted to work as corrections to the parton cascade. The first step is to see in which manner the dipole cascade could have produced the generated event.

For each event a possible chain of emissions is constructed, which can be seen as doing the inverse of a dipole cascade[1]. It is done by taking all the possible combinations of three partons that can be combined into two partons in accordance with the rules of the dipole cascade. This process is repeated until a number of possible chains of emissions have been reconstructed. For each emission $p^2_\perp$ is calculated.

Among the chains where $p^2_\perp$ is ordered, one chain is chosen at random weighted with the product of splitting functions of the reconstructed emissions. If no chains ordered in $p^2_\perp$ are found, an unordered chain is chosen.

The reconstructed states are labeled $S_0, ..., S_n$, where S_0 is the lowest order state and S_n is the state given by the matrix element. The corresponding scales are labeled $p^2_{\perp 1}, ..., p^2_{\perp n}$, where $p^2_{\perp i}$ is the scale at which state S_{i-1} emits a parton and evolves into state S_i.

There are two types of diagrams where the emissions cannot be reconstructed. They are simply events that ARIADNE could never generate. Examples of these two types of diagrams are shown in figure 8. There is still some uncertainty of how these should be dealt with. The annihilation diagram should probably be accepted as it is. It will not greatly effect any simulations since this type of diagram is very suppressed.

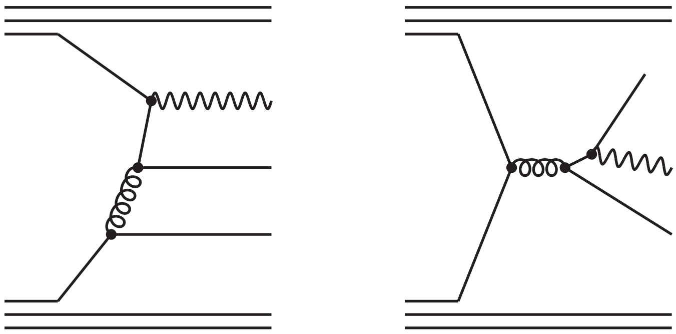

Figure 8: Diagrams showing processes that can not be produced in the ARIADNE cascade.

The other diagram is a bit more tricky. The best option is probably to add a new kind of emission reconstruction which is not present in ARIADNE and use the algorithm for matrix element matching in its present form. These diagrams are in need of further analysis before a method can be decided.

4.3 Sudakov Veto

The sum of the different jet ratios calculated from the matrix elements will be larger than one, since only the tree-level term in the matrix element is included. This is compensated by using Sudakov form factors.

Sudakov form factors correspond to the no emission probability for a state in a specific region of phase space. These factors can be approximated analytically or they can be introduced using Monte Carlo techniques. The Monte Carlo method works by generating an emission for the given state and checking if it ended up in the given region of phase space. This method is known as the Sudakov veto algorithm. The Monte Carlo method has the advantage that it is exactly what is implemented in the cascade, which makes the entire algorithm completely self consistent and should minimize any dependence on the cutoff.

First all intermediate states $S_0, ...S_{n-1}$ and scales $p^2_{\perp 1}, ..., p^2_{\perp n}$ are reconstructed according to the algorithm i section 4.2. Then for each intermediate state S_i one trial emission is made with $p^2_{\perp i+1}$ as starting scale. If the scale $p^2_{\perp}$ of the emission is above the next scale $p^2_{\perp i+1}$ in the reconstructed chain, the event is discarded. In this way all the Sudakov form factors are introduced since the probability to keep the event is exactly the probability of not having any emissions between the scales $p_{\perp i+1}^2$ and $p_{\perp i+1}^2$.

4.4 Running $\alpha_{\rm s}$

Matrix elements are calculated with a fixed $\alpha_{\rm s}$, whereas the cascades use a running $\alpha_{\rm s}$. When the cascade is reconstructed the invariant $p_\perp^2$ is calculated. This $p_\perp^2$ is used for calculating the $\alpha_{\rm s}$ that would have been used if the event had been generated by the cascade. The events are then reweighted using the factor $\Pi_{i=1}^n \alpha_{\rm s}(p_{\perp i}^2)/\alpha_{\rm sME}^n$, where n is the number of jets.

4.5 Reweighting Parton Distributions

The events generated by MadGraph are weighted with parton distributions using the momentum fractions for the entire hard sub-processes and the virtuality equal to the cutoff in the matrix element generation. Since these matrix elements are used to correct a cascade the events need to be reweighted with the distributions that would have been used in the cascade.

In the standard cascade the starting point is a generated lowest order event. The virtuality and momentum fractions of this lowest order event is used in the parton densities. For the corrected cascade the same approach is used. First all the emissions are reconstructed, which leads to a lowest order event. In this reconstructed state S_0 the virtuality and momentum fractions are calculated, which are used to reweight the event. In the case of W production the virtuality is going to be the mass of the W squared.

This gives the starting point of the cascade. In addition to this a factor is included for each reconstructed vertex. In the case of sea quark emission the factor is the ratio between the gluon and quark structure functions and in the case of gluon emission the soft cutoff present when an extended source takes part in the emission needs to be included. The explicit formulas for first order matrix element corrections are shown below. In order to present the complete formulas $\alpha_{\rm s}$ and Sudakov form factors are included. These factors are explained in section 4.3 and 4.4.

In a W plus no jets event generated by MadGraph, the event is weighted by the following:

$$xf_q(x_1, E_{cut}^2)xf_{q'}(x_2, E_{cut}^2)\sigma_{qq'} \tag{27}$$

$\sigma_{qq'}$ is the cross section for two quarks of flavor q and q' to form a W-boson. An ARIADNE event on the other hand would be weighted by:

$$xf_q(x_1, m_W^2)xf_{q'}(x_2, m_W^2)\sigma_{qq'}\Delta_{S_0}(s/4, E_{cut}^2) \tag{28}$$

This gives the following reweighted factor:

$$\frac{xf_q(x_1, m_W^2)}{xf_q(x_1, E_{cut}^2)} \cdot \frac{xf_{q'}(x_2, m_W^2)}{xf_{q'}(x_2, E_{cut}^2)}\Delta_{S_0}(s/4, E_{cut}^2) \tag{29}$$

In the case of W plus one jet events there has either been a gluon emission or a sea quark emission. In the case of a sea quark emission the events given by MadGraph have the following weight:

$$xf_g(x_1, E_{cut}^2)xf_{q'}(x_2, E_{cut}^2)P^{ME}(p_\perp^2, y)\alpha_{sME}\sigma_{qq'} \tag{30}$$

P^{ME} is the exact splitting function given by the matrix element, which is exactly what is to be factored out and used in ARIADNE for corrections.

When ARIADNE generates a sea quark event it has the following weight:

$$xf_q(x_1', m_W^2)xf_{q'}(x_2', m_W^2)P^{dip}(p_\perp^2, y)\frac{xf_g(x_1, p_\perp^2)}{xf_q(x_1', p_\perp^2)}\alpha_s(p_\perp^2)\sigma_{qq'}\Delta_{S_0}(s/4, p_\perp^2) \tag{31}$$

x_1' and x_2' are the reconstructed momentum fractions and Δ denotes the Sudakov form factor. In order to factor out the correct splitting function from the matrix element the following reweighting factor is used.

$$\frac{xf_q(x_1', m_W^2)}{xf_g(x_1, E_{cut}^2)} \cdot \frac{xf_{q'}(x_2', m_W^2)}{xf_{q'}(x_2, E_{cut}^2)} \cdot \frac{\alpha_s(p_\perp^2)}{\alpha_{sME}} \cdot \frac{xf_g(x_1, p_\perp^2)}{xf_q(x_1', p_\perp^2)}\Delta_{S_0}(s/4, p_\perp^2) \tag{32}$$

In the case of a gluon emission MadGraph gives events weighted with the following:

$$xf_q(x_1, E_{cut}^2)xf_{q'}(x_2, E_{cut}^2)P^{ME}(p_\perp^2, y)\alpha_{sME}\sigma_{qq'} \tag{33}$$

A sea quark event generated by ARIADNE has the following weight:

$$xf_q(x_1', m_W^2)xf_{q'}(x_2', m_W^2)P^{dip}(p_\perp^2, y)\theta(p_\perp^2, y)\alpha_s(p_\perp^2)\sigma_{qq'}\Delta_{S_0}(s/4, p_\perp^2) \tag{34}$$

θ is the suppression from the extendedness of the proton remnants discussed in section 3.5.

Comparing the pole structure of the dipole splitting function with that of the matrix element an extra $1/z$ pole is found because of the fact that the dipole splitting is a final state process while the matrix element describes an initial state gluon emission.

$$\frac{P_g^{ME}(p_\perp^2, y)}{z} \approx P_g^{dip}(p_\perp^2, y) \tag{35}$$

Therefore the reweighting factor for gluon events is the following:

$$\frac{xf_q(x_1', m_W^2)}{xf_q(x_1, E_{cut}^2)} \cdot \frac{xf_{q'}(x_2', m_W^2)}{xf_{q'}(x_2, E_{cut}^2)} \cdot \frac{\alpha_s(p_\perp^2)}{\alpha_{sME}} \cdot \frac{\theta(p_\perp^2, y)}{z} \Delta_{S_0}(s/4, p_\perp^2) \tag{36}$$

This method can be used for any arbitrary number of jets. First the structure functions are reweighted to that of the reconstructed lowest order event, and then multiplied by the appropriate reweighting factor for each reconstructed vertex.

4.6 The Algorithm

All the necessary pieces have been presented above. It is a matter of putting them all together in a scheme useful for generating events. The whole algorithm is the following:

1. Generate a large number of events using MadGraph. The events generated contain a W^+ and between zero and N jets. Each event is above a specific cutoff defined by the $k_\perp$-clustering algorithm. The events are weighted according to their cross section. The weight is the cross section for the specific jet multiplicity divided by the number of events with that multiplicity.

2. Now use the algorithm described in section 4.2 to construct all the intermediate states $S_0, ...S_{n-1}$ and the corresponding scales $p_{\perp 1}^2, ..., p_{\perp n}^2$.

3. Use the reconstructed scales to reweight the event with a running α_s according to the method in section 4.4.

4. Reweight the parton densities and a reweighting factor for each vertex according to the method described in section 4.5.

5. For each reconstructed state S_i perform a trial emission with $p_{\perp i}^2$ as starting scale. If the emission has a $p_\perp^2$ higher than $p_{\perp i+1}^2$ the event is discarded.

6. For the trial emission from state S_n.

(a) If the jet multiplicity of the event is the maximum (n=N), accept the event and trial emission.

(b) If the event has a jet multiplicity below the maximum, check if the trial emission was above the matrix element cutoff. If it was above the cutoff discard the event, otherwise accept the event and the trial emission.

7. Continue the parton cascade.

5 Results

All the simulations are done with proton antiproton collisions at the energy of the Tevatron, which is 1960GeV, and the process studied is W^+-production.

The first and foremost test of the algorithm that needs to be done is to make sure that it is really self consistent. The result should be weakly dependent on the chosen cutoff. The standard ARIADNE cascade reproduces the first order matrix element to begin with, so to start off ARIADNE is compared to ARIADNE corrected with only first order matrix elements. The events used in ARIADNE without correction are the MadGraph zero jet events. This ensures that cross section and W-mass distribution in the two simulations are identical. To study the detailed properties of the algorithm the simulation is split up into the case where the first emission was a gluon and where it was a sea quark. To test the algorithm the transverse momentum spectrum of the W-boson is used.

The cutoff used in the simulation was the $k_\perp$-clustering algorithm described in section 2.4. The algorithm used is covariant E-scheme with a 10GeV cutoff. Unfortunately there exist a numerical instability in the structure function reweighting, which needs to be minimized by the introduction of further matrix element cuts. The instability is due to that the parton density of the original event can be very small compared to the reconstructed density especially at large x. This introduces very large reweighting factors. The way to resolve this issue is to rerun MadGraph with a flat distribution function. This was not done due to lack of time. Instead steps were taken to minimize the problem. All the matrix element generated events with at least one jet that has a pseudorapidity above 2.5 were excluded. This removes some of the corrections from the matrix elements but excludes the area of phase space where most of the large reweighting factors appear. In the excluded area of phase space jets are generated with the ARIADNE cascade instead. The

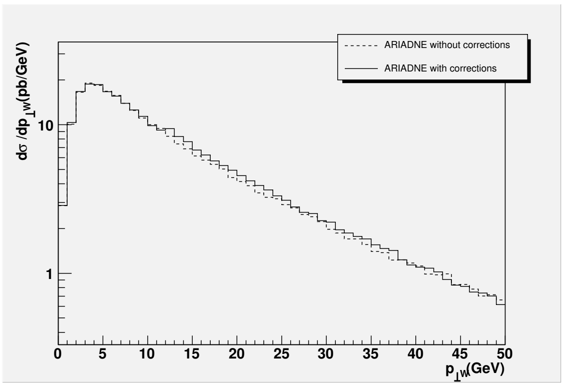

Figure 9: Transverse momentum of the W when the first emission is a sea quark.

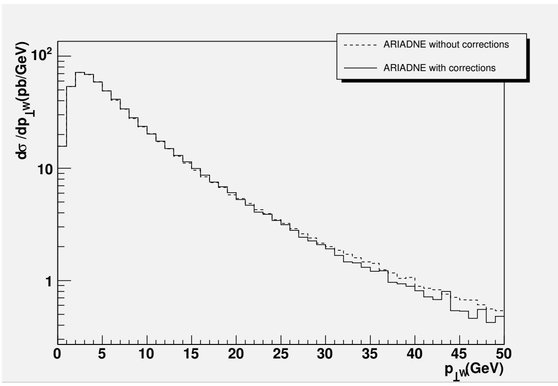

Figure 10: Transverse momentum of the W when the first emission is a gluon.

corrections that are excluded by this extra cutoff only effect jets that would not have been detected at the Tevatron.

The results indicate that the algorithm is working in the sea quark case, shown in 9. The figure shows a nice agreement between the curves except close to the cutoff. The reason for this discrepancy still puzzles the author.

In the gluon emission case the histogram, shown in figure 10, shows good agreement except for high transverse momenta. The reason for the differences at high transverse momenta may be a flaw in the calculations of the first order gluon emission in ARIADNE. This flaw makes the calculations inaccurate for high rapidity and high transverse momenta. A histogram containing all the events is shown in figure 11.

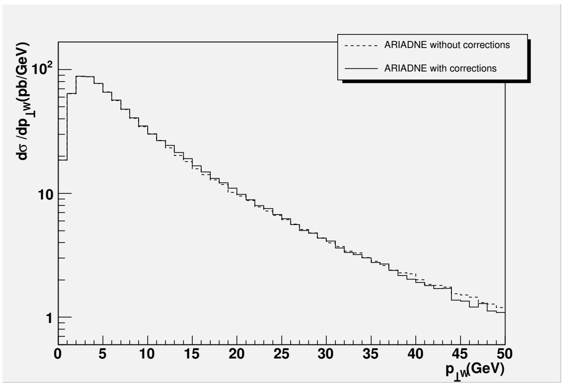

Figure 11: Transverse momentum of the W for all events.

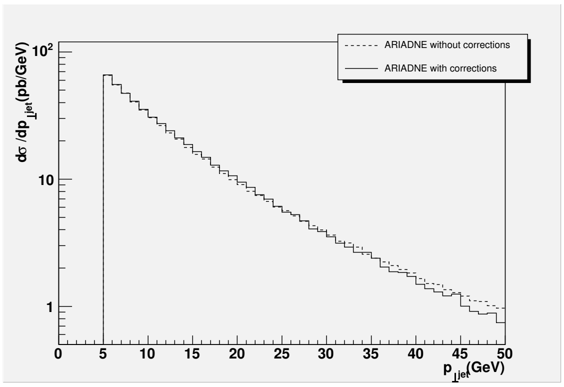

Figure 12: Transverse momentum for the first jet.

Further consistency checks include studying the properties of the first jet, defined as the one with largest transverse momenta. To define the jets the same scheme as in the matrix element cutoff is used, namely the covariant E-scheme but this time with a 5 GeV cutoff. The cutoff is set a bit lower to see if there are any discrepancies close to the matrix element cutoff. The transverse momentum for the first jet is shown in figure 12 and the rapidity of the first jet in figure 13. Both these histograms show good agreement.

Unfortunately due to lack of time no simulations with higher order matrix element corrections are presented at this time.

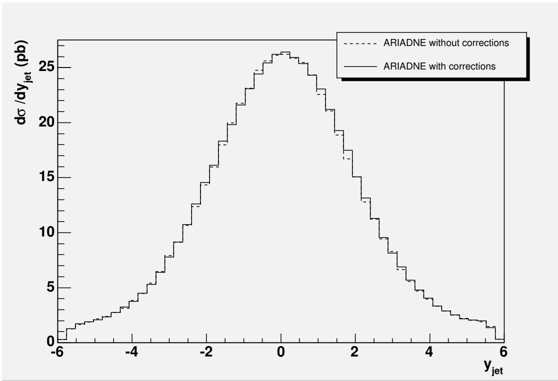

Figure 13: Rapidity of the first jet.

6 Conclusions

This thesis described a way of correcting ARIADNE with higher order matrix elements in hadronic collisions. In order to adapt the correction algorithm used in the e^+e^- case, several parts need to be extended. First new clustering schemes and their splitting functions need to be implemented for sea quark emission and emission from an extended source.

A new scheme for reweighting the parton densities was constructed and implemented. The reweighting is not just needed for an event as a whole, but also for each vertex. This has been done for first order matrix elements and it is clear how this scheme should be extended to higher jet multiplicity, but a little work is needed verifying the formulas when more vertices are present.

The algorithm was tested by simulating W production at the Tevatron. It is working for first order corrections, but there are still some flaws that need to be sorted out before proceeding to higher jet multiplicity.

References

[1] L. Lönnblad, "Correcting the colour-dipole cascade model with fixed order matrix elements," JHEP **0205** (2002) 046 [arXiv:hep-ph/0112284].

[2] L. Lönnblad, "ARIADNE version 4: A Program for simulation of QCD cascades implementing the color dipole model," Comput. Phys. Commun. **71** (1992) 15.

[3] G. Gustafson and U. Pettersson, "Dipole Formulation Of QCD Cascades," Nucl. Phys. B **306** (1988) 746.

[4] B. Andersson, G. Gustafson, L. Lönnblad and U. Pettersson, "Coherence Effects In Deep Inelastic Scattering," Z. Phys. C **43** (1989) 625.

[5] L. Lönnblad, "Small x effects in W + jets production at the Tevatron," Nucl. Phys. B **458** (1996) 215 [arXiv:hep-ph/9508261].

[6] B. Andersson, G. Gustafson, G. Ingelman and T. Sjöstrand, "Parton Fragmentation And String Dynamics," Phys. Rept. **97** (1983) 31.

[7] S. Catani, Y. L. Dokshitzer, M. H. Seymour and B. R. Webber, "Longitudinally invariant K(t) clustering algorithms for hadron hadron collisions," Nucl. Phys. B **406** (1993) 187.

[8] J. Pumplin, D. R. Stump, J. Huston, H. L. Lai, P. Nadolsky and W. K. Tung, "New generation of parton distributions with uncertainties from global QCD analysis," JHEP **0207** (2002) 012 [arXiv:hep-ph/0201195].

[9] T. Stelzer and W. F. Long, "Automatic Generation Of Tree Level Helicity Amplitudes," Nucl. Phys. Proc. Suppl. **37B** (1994) 158.

[10] H. Murayama, I. Watanabe and K. Hagiwara, "HELAS: HELicity amplitude subroutines for Feynman diagram evaluations," KEK-91-11